Proceedings of the 5th International Conference on Fluid Flow and Thermal Science (ICFFTS 2024)
Lisbon, Portugal- November 21 - 23, 2024
Paper No. 133
DOI: 10.11159/icffts24.133

Piecewise Viscous Drag Coefficient Calibration Methodology for Floating Platform Heave Free Decay Test in Full-Scale CFD Simulation.

Miguel Gil[1], Javier Armañanzas[1], Juan Pablo Fuertes[1], Alexia Torres[1], Javier Leon[1]
[1]Public University of Navarra
Av. Cataluña S/N, Pamplona, Spain
miguel.gil@unavarra.es; javier.armananzas@unavarra.es; juanpablo.fuertes@unavarra.es; alexia.torres@unavarra.es; javier.leon@unavarra.es

Abstract – In this paper, a new methodology is developed to establish the drag coefficient of the floating offshore platform DeepCWind, applied in full-scale CFD simulations. A software based on the Lattice Boltzmann method implemented in Simulia Xflow 2023x is used. This methodology aims to faithfully represent the heave damping in high altitude free decay test, where the velocities reached by the platform are high and where models with constant coefficient overpredict the damping. A calibration process is performed to define a piecewise function for the viscous drag coefficient. Due to the lack of experimental data, the calibration is performed against a simulation model based on potential-flow method and including a quasi-static mooring system. In this way, the mean square error is reduced and the natural period of the system is adjusted.

***Keywords*:** CFD, Drag, Viscous, DeepCWind, Free decay

1. Introduction

The usage of analytical model based software's for the hydrodynamic simulation of floating offshore platforms in wind industry is an increasing resource among researchers in this area. This methodology proposes solutions that are able to predict the behaviour of wind turbines under aerodynamic, wave and mooring loads among others, with a reduced computational cost. However, it has been shown that the Blade Element Momentum method implemented in FAST has limitations in capturing the interaction between the wind turbine and the wake, especially at low frequency excitations [1].

High fidelity floating wind turbine simulations based on Computational Fluid Dynamics (CFD) in co-simulation with Finite Element Method (FEM) software are intended to be able to represent certain instabilities that cannot be captured by analytical models, achieving a more realistic representation of the wind turbine behaviour.

Several studies have shown that CFD models are able to represent the 3 main effects involved in the hydrodynamic behaviour of FOWTs; added mass [2], wake radiation [3] and viscous effects [4]. Viscous effects are difficult to represent, as they require a mesh size small enough to obtain a non-dimensional wall distance value $y^+ < 1.5$ [5], and where the boundary layer is realistically represented, with the consequent computational cost. Reducing the mesh size to tenths of a millimetre in simulations with 1/50 scale models is feasible in terms of computational cost, but unfeasible in full-scale simulations, even more in the selected CFD simulation software, where refinement methods can not be applied to simple elements but to the whole structure. Therefore, it is not possible to correctly represent viscous effects in full-scale models and it is necessary to resort to analytical models to represent this effect.

In Phase II of OC4 project [6] the introduction of an additional drag force by means of a Quadratic Drag model is proposed, and a drag coefficient valid for simulation models based on potential flow is established. As will be discussed later, this drag coefficient does not apply to CFD models and contradicts the value proposed in [7]. In this paper we have analysed the effect of this drag coefficient and a new methodology to correctly representing the viscous stresses by means of a piecewise time-dependent function is proposed.

Validating this methodology implies obtaining experimental results from full-scale models, which entails a high economic cost. Therefore, in order to test the validity of this methodology, the CFD model will be validated with respect to results present in the literature extracted from potential flow models. For this purpose, a software based on the Lattice Boltzmann method, Simulia XFlow 2023x, will be used.

2. Loadcase

The study focuses on the heave degree of freedom, as this is the main damping motion of the platform, and the one for which the heave plates are designed. However, this study can be applied to any degree of freedom of the platform, taking into account that for sway and surge motion, mooring system plays a key role.

2.1. Floating platform

A heave free decay of 6 m above the draft level of the DeepCWind platform is performed, the properties of which are presented in Table 1. This load case corresponds to 1.3b of OC4 project, Task 30 [8], for which the results of numerous simulation models based on potential flow theory are known. The simulation is performed in still water and no air condition.

A static equilibrium calibration process is performed, and it is decided to modify the initial draft point to 18.47 m from the theoretical 20 m. In this way, the properties of the mooring lines and the mass of the platform are not altered, which could have led to changes in the natural frequency of the system.

Table 1: Structural properties of floating platform

Property	**Value**	**Units**
Total draft	18.47	m
Platform mass, including ballast	1.3473e7	kg
Platform center of mass (CM) under SWL	7.53	m
Platform roll inertia about CM	6.827e9	$kg \cdot m^2$
Platform pitch inertia about CM	6.827e9	$kg \cdot m^2$
Platform yaw inertia about CM	1.226e10	$kg \cdot m^2$

2.2. Mooring System

The simulation carried out by XFlow is performed with a Quasi-Static mooring system, implemented according to the equations described in [9]. Therefore, the results will be compared with a model where the mooring system is also Quasi-Static, although the differences with a dynamic model are practically negligible. The platform has a mooring system composed of 3 catenary-shaped lines, forming an angle of 120º between them and whose characteristics are shown in Table 2. The mooring of each of the lines is done in each of the base columns, which corresponds to a Multi-Point Mooring arrangement.

Table 2: Mooring System properties

Property	**Value**	**Units**
Distance from fairleads to the center of the platform	40.868	m
Distance from anchors to the center of the platform	837.6	m
Total chain length	835.5	m
Line diameter	0.0766	m
Axial stiffness	753.6	MN
Lineal density	113.35	kg/m
Lineal density in water	108.63	kg/m

3. Computational domain

Simulia XFlow employs a meshing system based on the Lattice Boltzmann method, where the elements are cube-shaped. By defining the element size of a mesh level by the edge of that cube, the element size of the next higher level has an element size corresponding to twice the element size.

3.1. Grid

Two different meshes are studied, keeping the element size of the lower level (Target Resolved Scale) at 0.22 m, and varying the total number of mesh levels, at 3 and 4. Thus, Mesh 1 has a global mesh size (Resolved Scale) of 0.88 m, while Mesh 2 has 1.76 m. The Refinement Transition Length (RTL) sets the number of elements that make up the thickness of a mesh level before increasing to the next level, and is maintained at 6 for both meshes. For both cases the Time Step is kept at 0.0125 s, which corresponds to TN/700, TN being the theoretical natural period of the system.

Fig. 1 shows an image of the mesh used.

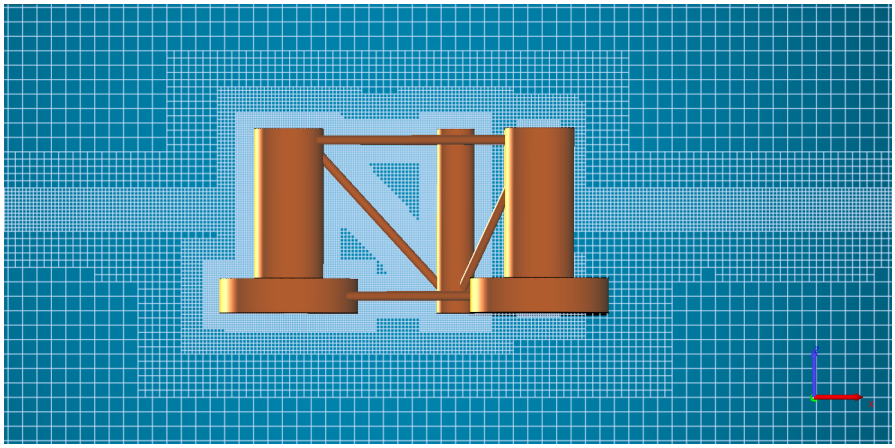

Fig. 1: Mesh sample corresponding to Grid 2.

3.2. Boundary conditions

The boundary conditions on the wall of the geometry that comes in contact with the fluid can alter the hydrodynamic behaviour of the platform. The wall boundary condition for the selected mesh causes a small damping with respect to the free slip condition, but in no case represents the viscous damping. Therefore, and to avoid redundancy, it is necessary to set the boundary condition as free slip. Fig. 2 shows the impact on the damping as a function of the boundary conditions.

This figure not only shows the importance of boundary condition, but also the need of implementing a system for the correct representation of viscous drag in order to increase heave damping.

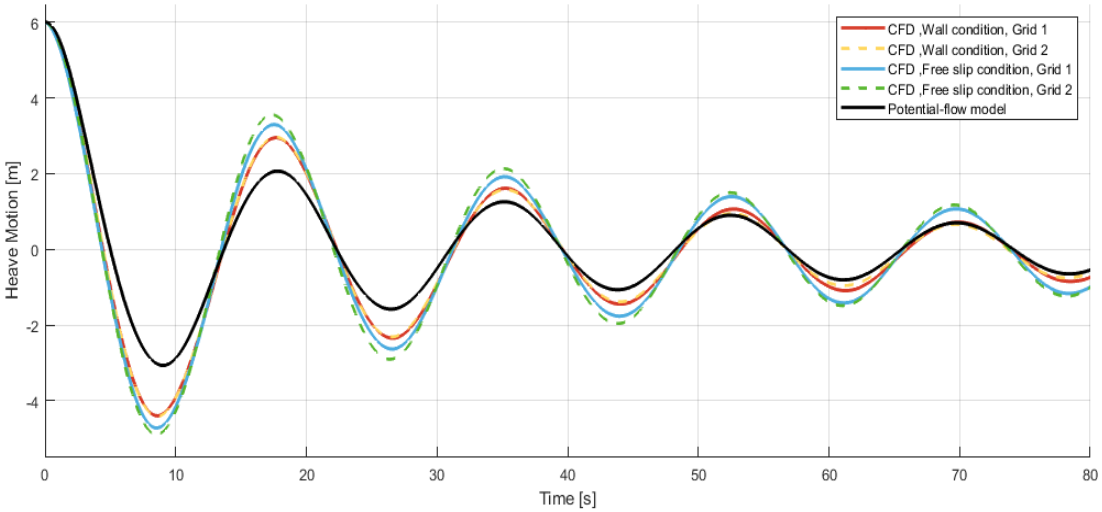

Fig. 2: Influence of boundary condition under heave free decay test.

4. Theorical viscous drag model

In [6] it is shown the necessity of introducing a viscous damping by means of Quadratic Drag, in case the viscous effect is not studied correctly by the simulation software. This additional drag forze is stablished by Eq (1), where B_{ij}^{quad} is the damping coefficient and $\dot{q}_j$ determines the relative velocity of the platform with respect to the fluid in a specific degree of freedom.

$$F_i^{Additional\ Drag}(\dot{q}) = -B_{ij}^{quad}\left|\dot{q}_j\right|\dot{q}_j \tag{1}$$

On the one hand, [6] determines B_{ij}^{quad} by comparing free decays motion of a potential-flow based simulation model to a potential-flow model implemented with the Morison's viscous term. For heave degree of freedom, B_{heave}^{quad} = 3.88e6 Ns²/m².

On the other hand, [7] establishes the drag coefficients of the elements that conform the DeepCWind platform implemented in OpenFast, resulting in a B_{heave}^{quad} = 2.78e6 Ns²/m².

The difference between the values in viscous damping coefficient causes a noticeable difference in the behaviour of the platform, as depicted in Fig. 3. Furthermore, for the case where B_{heave}^{quad} = 2.78e6 Ns²/m², the damping setting at the first drop is closer to the behaviour of the potential flow models. However, for the following instants, the damping is excessive, which leads to think that the quadratic drag should not be constant throughout the simulation.

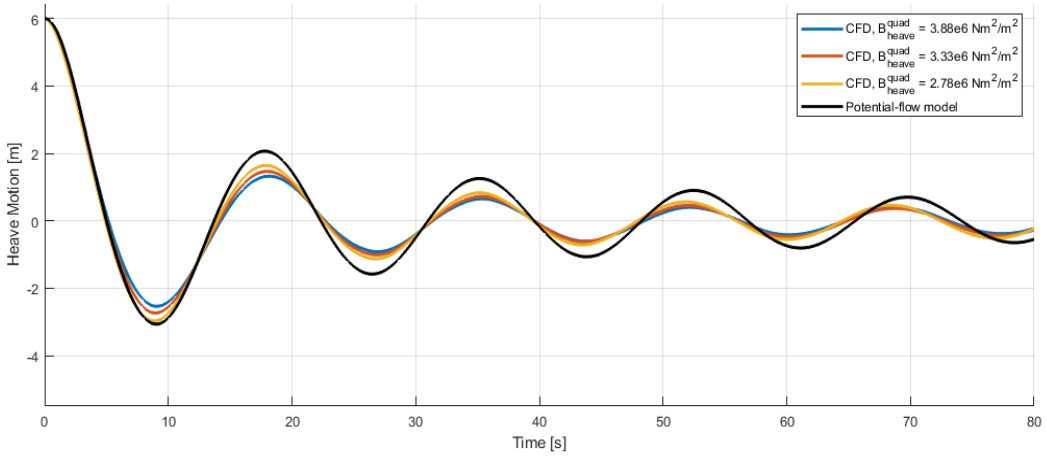

Fig. 3: Effect of viscous drag in heave free decay

5. Variable viscous drag model

According to results present in Fig. 3, it is observed that viscous effects plays a key role in the first and second damping cycle. In the rest of the simulation, the velocity reached by the platform is low, and the viscous effect does not make much difference in damping. Therefore, from the second cycle onwards, the drag coefficient can be kept constant and this will not cause a large error in the simulation.

In order to correctly adjust the damping in the first cycle, it is divided into two regions; falling region and elevation region.

5.1. Falling region

The falling region corresponds to the instants between 0 < t < 8.9 s, being t the simulation time. The initial position of the platform is +6 m with respect to the draft position, and according to the reference model, a damping amplitude of 9.07 m is intended to be achieved, until the platform is positioned at -3.07 m.

Different cases are simulated, varying B_{ij}^{quad} from 2.25e6 Ns²/m² up to 3.0e6 Ns²/m², at intervals of 2.5e5 Ns²/m², and the vertical position of the platform is monitored over time. The results are presented in Fig. 4, in comparison with the Potential Flow based simulation.

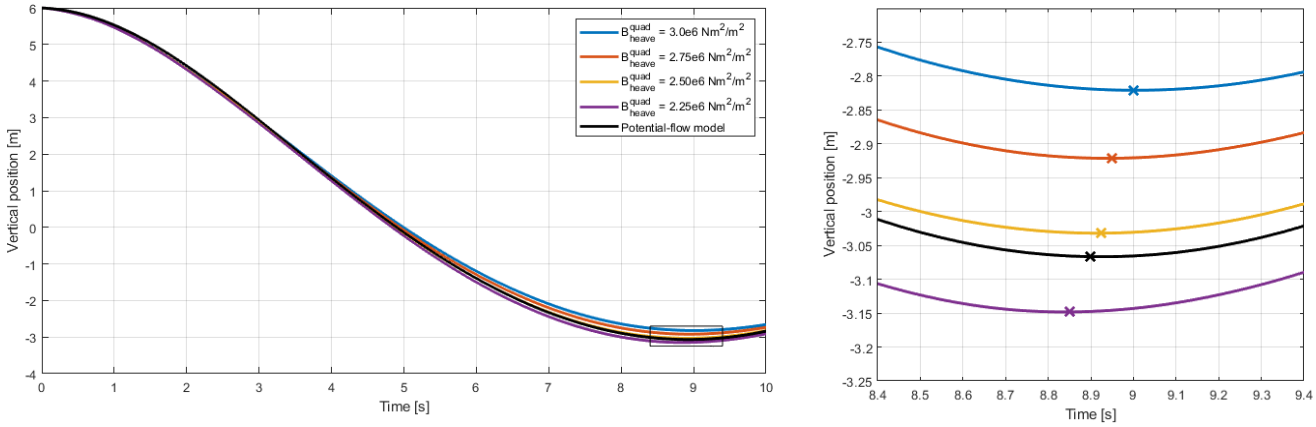

Fig. 4: Effect of drag coefficients on heave damping in falling region (left) and detail view of minimum elevation (right).

Table 3 shows the minimum heave position of the platform as a function of the Drag Coefficient. In order to determine and calibrate the model achieving a minimum position of -3.067 m, a linear regression process has been made, resulting in B_{ij}^{quad} = 2.46e6 Ns²/m².

Table 3: Minimum position of platform motion as a function of Drag Coefficient in Falling process

Model	Minimum position [m]	Drag Coefficient [Ns²/m²]
CFD Simulation	-2,821	3,00E+06
	-2,921	2,75E+06
	-3,032	2,50E+06
	-3,148	2,25E+06
Reference	**-3,067**	**2,46E+06**

5.1. Elevation region

The falling region corresponds to the instants between 8.9 < t < 17.4 s. By simplification, the initial position of the platform is -3 m with respect to the draft position, and a damping amplitude of 5.06 m is intended to be achieved, until the platform is at 2.06 m. However, this induces an error that may justify a possible mismatch in the final behaviour of the vessel.

Different cases are simulated, varying the B_{ij}^{quad} from 1.5e6 Ns²/m² up to 2.7e6 Ns²/m², at intervals of 2e5 Ns²/m², and the vertical position of the platform is monitored over time. The results are presented in Fig. 5, in comparison with the Potential Flow based model.

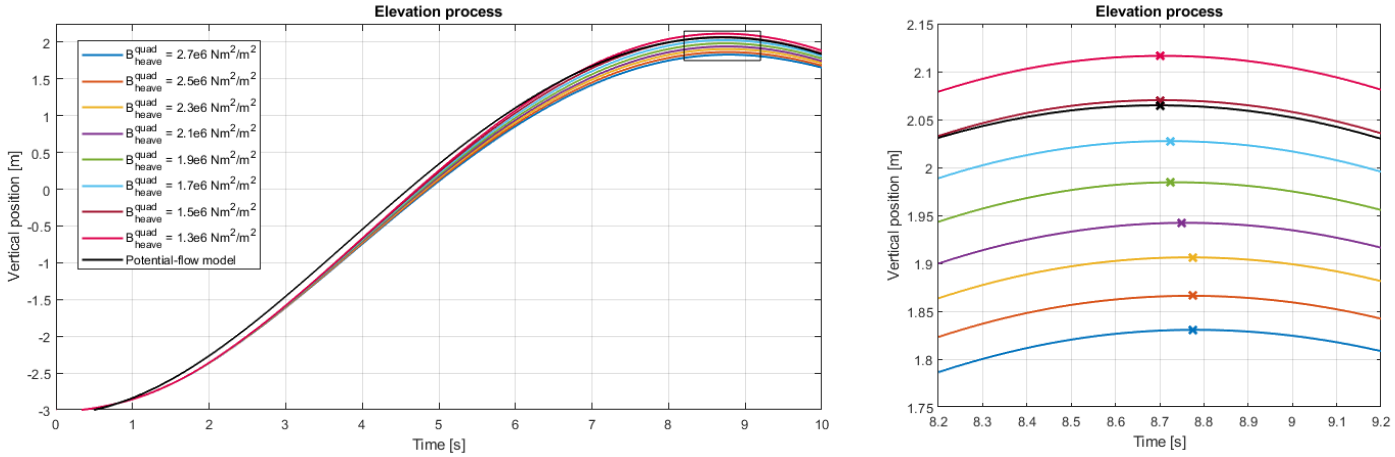

Fig. 5: Effect of drag coefficients on heave damping in elevation region (left) and detail view of maximum elevation (right).

The same process described above has been made for the Elevation process, estimating B_{ij}^{quad} = 1.53e6 Ns²/m². Regression process is made according to values described in Table 4.

Table 4: Maximum position of platform motion as a function of Drag Coefficient in Elevation process

Model	Maximum position [m]	Drag Coefficient [Ns²/m²]
CFD Simulation	1,830	2,70E+06
	1,866	2,50E+06
	1,906	2,30E+06
	1,942	2,10E+06
	1,984	1,90E+06
	2,027	1,70E+06
	2,070	1,50E+06
	2,116	1,30E+06
Reference	**2,065**	**1,53E+06**

5.3. Piecewise function, validation model.

According to results presented in section 5.1 and 5.2, the selected piecewise function of B_{ij}^{quad} as a function of time is presented in Eq (2).

$$B_{heave}^{quad}(t) = \begin{cases} 2.46e6\ Ns^2/m^2\ , & 0 < t < 8.9\ s \\ 1.53e6\ \ Ns^2/m^2, & t > 8.9\ s \end{cases} \quad (2)$$

Fig. 6 shows the resulting damping behaviour of the platform, compared to the models where the drag coefficient is constant, and to the potential flow model with which it is intended to be validated. With this model, the heave behaviour of the platform is similar to the potential flow model, not only in amplitude but also in its natural period, where the error is less than 0.4%, compared to the 1.5% error in the period of the model with constant drag coefficient.

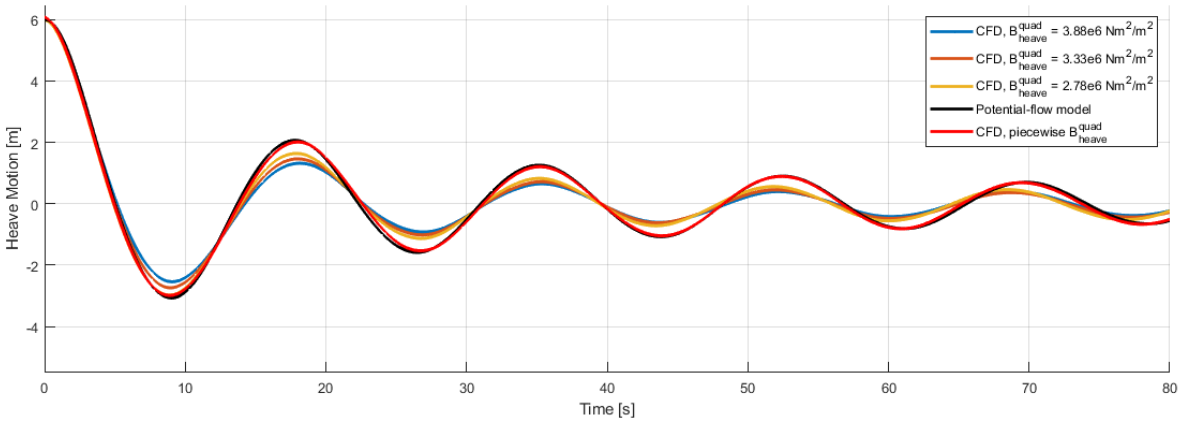

Fig. 6: Platform heave damping behavior for piecewise quadratic drag coefficient function.

The mean square error (MSE) of the heave position of the CFD simulation models versus the reference model is analyzed. The simulation using the coefficient proposed in [6] shows an $MSE_1 = 0.157$ m^2, while in the one proposed in [7] the $MSE_2 = 0.073$ m^2. A great improvement in terms of ECM is observed when a variable drag coefficient model is used, obtaining an $MSE_3 = 0.0057$ m^2, which supposes an improvement of 96.2 % with respect to model 1 and 92.1 % with respect to model 2.

6. Conclusions

In this paper, a new methodology is presented to validate a free decay model in the heave degree of freedom for a full-scale CFD model. It is necessary to introduce an analytical model that allows to represent faithfully and, in the whole range of motion, the viscous stresses that take place. Models proposing a constant drag coefficient overpredict the damping especially in the first cycle, where the platform velocities are high. Therefore, it is necessary to introduce a time-varying function.

A study has been carried out to analyse the effect of the drag coefficient on the damping, observing less damping as the drag coefficient is reduced. This allows the coefficient to be calibrated to adapt the behaviour to a particular model and to validate the CFD simulation model. The calibration process is separated into 2 half-periods, as it is found to be sufficient to represent the behaviour with a low mean square error.

The drag coefficient not only has an effect on the damping, but also on the natural period of the system. By means of this technique it has been possible to reduce the error in the natural period, obtaining an error of 0.4 %, and to reduce the MSE by 92.1 % with respect to constant coefficient models with values present in the literature. This methodology can be applied in all degrees of freedom of the platform, being especially effective in those where viscous effects are considerable.

The mesh size and the time step used in the CFD simulation are key parameters to correctly capture the behaviour of the platform. Therefore, before performing the drag coefficient calibration it is necessary to perform a mesh convergence test, and assure that the only error in the behaviour can be attributable to viscous stresses.

Acknowledgements

The authors acknowledge the support from the Government of Navarre (Research project: PC042-043 COSTA)

References

[1] C. W. Schulz, U. Özinan, S. Netzband, P. W. Cheng y M. Abdel-Maksoud, «The Impact of Unsteadiness on the Aerodynamic Loads of a Floating Offshore Wind Turbine,» *Journal of Physics: Conference Series,* vol. 2626, nº 1, p. 012064, 2023.

[2] Y. Yang , M. Bashir, C. Michailides, C. Li y J. Wnag, «Development and application of an aero-hydro-servo-elastic coupling framework for analysis of floating offshore wind turbines,» *Renewable Energy,* vol. 161, pp. 606-625, 2020.

[3] H. Yang y W. Decheng, «Investigation of Interference Effects Between Wind Turbine and Spar-Type Floating Platform Under Combined Wind-Wave Excitation,» *Sustainability,* vol. 12, nº 1, 2020.

[4] A. Ortolani, G. Persico, J. Drofelnik, A. Jackson y S. M. Campobasso, «Computational Fluid Dynamics Analysis of Floating Offshore Wind Turbines in Severe Pitching Conditions,» *Journal of Engineering for Gas Turbines and Power,* vol. 142, nº 12, p. 121003, 11 2020.

[5] S. Burmester, G. Vaz, S. Gueydon y O. El Moctar, «Investigation of a semi-submersible floating wind turbine in surge decay using CFD,» *Ship Technology Research,* vol. 67, nº 1, pp. 2-14, 2020.

[6] A. Robertson, J. Jonkman, M. Masciola, H. Song, A. Goupee, A. Coulling y C. Luan, «Definition of the Semisubmersible Floating System for Phase II of OC4,» 9 2014.

[7] A. Srinivas, B. Bobertson, J. B. Gadasi, B. G. Simpason, P. Lomónaco y J. M. Ilzarbe, «Impact of Limited Degree of Freedom Drag Coefficients on a Floating Offshore Wind Turbine Simulation,» *Journal of Marine Science and Engineering,* vol. 11, nº 1, 2023.

[8] A. Robertson, J. Jonkman, F. Vorpahl, W. Popko, J. Qvist, L. Frøyd, X. Chen, J. Azcona, E. Uzunoglu, C. Guedes Soares, C. Luan, H. Yutong, F. Pengcheng, A. Yde, T. Larsen, J. Nichols, R. Buils, L. Lei, T. A. Nygaard, D. Manolas, A. Heege, S. R. Vatne, H. Omberg, T. Duarte, C. Godreau, H. F. Hansen, A. W. Nielsen , H. Riber, C. Le Cunff, F. Beyer, A. Yamaguchi, K. J. Juang, H. Shin, W. Shi, H. Pasrk, M. Alves y M. Guérinel, «Offshore Code Comparison Collaboration Continuation Within IEA Wind Task 30: Phase II Results Regarding a Floating Semisubmersible Wind System,» de *International Conference on Ocean, Offshore and Arctic Engineering*, California, 2014.

[9] M. Masciola, J. Jonkman y A. Robertson, «Implementation of a Multisegmented, Quasi-Static Cable Model,» de *International Ocean and Polar Engineering Conference*, Alaska, 2013.